

# Impact of High-Temperature Heat Treatment on the Microstructure of Ti-Mo Alloys (Ti-6Al-4V)

Amira S. Hassan, Khaled A. M. Attia

Egyptian Academy of Engineering and Technology, Cairo, Egypt

**Abstract**—The present study was undertaken to investigate the effect of aging parameters (time and temperature) on the mechanical properties of Be-and/or Zr- treated Al-Mg-Zn (7075) alloys. Ultimate tensile strength, 0.5% offset yield strength and % elongation measurements were carried out on specimens prepared from cast and heat treated 7075 alloys containing Be and/or Zr. Different aging treatment were carried out for the as solution treated (SHT) specimens (after quenching in warm water). The specimens were aged at different conditions; Natural and artificial aging was carried out at room temperature, 120C, 150C, 180C and 220C for different periods of time. Duplex aging was performed for SHT conditions (pre-aged at different time and temperature followed by high temperature aging). Ultimate tensile strength, yield strength and % elongation data results as a function of different aging parameters are analysed. A statistical design of experiments (DOE) approach using fractional factorial design is applied to acquire an understanding of the effects of these variables and their interactions on the mechanical properties of Be- and/or Zr- treated 7075 alloys. Mathematical models are developed to relate the alloy mechanical properties with the different aging parameters.

**Keywords**—Casting, Aging Treatment, Mechanical Properties, Al-Mg-Zn (7075) alloys, Be- and/or Zr-Treatment, Experimental Correlation.

## I. INTRODUCTION

HIGH strength Al-Zn-Mg-Cu (7XXX series) alloys are extensively used in the aerospace industry, where newer materials with high specific properties are always in high demand. The addition of Zr produces a significant improvement in the tensile properties as a result of its grain refining action. In addition to refining the grain size of the Al alloys during casting, Zr additions also increase the resistance to recrystallization during hot working and contribute to further strengthening by the formation of fine coherent Al<sub>3</sub>Zr dispersoids [1]-[5]. Accordingly, the maximum benefit from Zr additions is obtained by producing a supersaturated solid solution of these elements during casting, which is then decomposed to produce a high number density of fine Al<sub>3</sub>Zr dispersoids during controlled heat treatment. The increments in strength can be attributed to grain refining and substructure strengthening as well as dispersion hardening.

Youdelis and Fang [6] investigate the effect of beryllium on age hardening, defect structure, and S' formation in the Al-2.5Cu-1.2Mg alloy. Their results show that addition of 0.15%Be significantly increases the peak hardness and overall precipitation rate for the Al-2.5Cu-1.2Mg alloy. In another study, the effect of micro-additions of Be on the aging behaviour of Al-0.75Mg-0.5Si alloy was investigated by [7]. The results show that addition of 0.1%Be significantly increases the hardening rate

and the maximum hardness level attainable when the alloy is aged at various temperatures from room temperature to 300°C. Optical and scanning electron microscopical observations show a significantly higher precipitate density for the Be containing alloy when compared with the base Al-Mg-Si alloy.

Wang et al. [8] investigate the effects of beryllium (Be) and solution temperature on the morphologies of iron intermetallics, silicon particles, and copper intermetallics, relative to the mechanical properties of 319.0 alloys. Their experimental results indicated that adding Be to the alloy can raise the Al-Al<sub>2</sub>Cu eutectic melting temperature, change some platelet-like shape ( $\beta$ -Al<sub>5</sub>FeSi) of iron intermetallics to comparatively harmless Chinese-script morphologies ( $\alpha$ -Al<sub>3</sub>Fe<sub>2</sub>Si), and reduce the amount and average length of  $\beta$ Al<sub>5</sub>FeSi platelets. Fractographic analysis of tested compact tension specimens revealed that the fracture processes were mainly initiated by void nucleation at  $\beta$ -Al<sub>5</sub>FeSi platelets as a result of their cracking and decohesion from the matrix. Adding Be to the 319.0 alloy and optimizing the solution temperature could significantly decrease the number of fracture-initiation sites of  $\beta$ -Al<sub>5</sub>FeSi platelets and improve the tensile properties and fracture toughness.

Strength of 7075 alloy is mainly controlled by the aging process of precipitation and growth of very fine precipitates of the  $\eta'$  phase (MgZn<sub>2</sub>). In Al/Zn/Mg alloy, it was found that storage at room temperature before heat to the aging temperature leads to the formation of finer precipitate structure and better properties. Duplex aging enhances corrosion resistance since the grain boundary zone is removed. The 7075 alloy also demonstrates a high response to age hardening [9]-[11]. Aging at 120°C for 24hs was recommended for 7075 alloys [8]-[12]. Retrogression and reaging (RRA) are expected to optimize the 7000 alloy series tensile properties. The RRA sequence after solution heat treatment and quenching in cold water is: i) T6 aging, 120°C/24h, ii) short time heating, 200-250°C/5-10min, followed by cold water quenching and iii) T6 re-aging, 120°C/24h [13], [14]. Many studies [15]-[20] focused on the effect of heat treatment on 7075 alloys. Increases in the strength of the 7075 alloy are believed to arise mainly from the fine dispersion of small  $\eta$  particles [17]. The microstructure of the grain boundary particles which depend on the aging process is the main parameter controlling the 7075 alloy mechanical properties. The high strength of this alloy in the RRA temper is considered to arise from both the presence of many fine  $\eta$  particles, which are probably coherent, and of the high overall concentration of particles in this structure [19].

Age hardening heat treatment operation was found to improve yield strength and ultimate tensile strength values but lower ductility. On the other hand, annealing heat treatment operation improves ductility but lower yield strength and ultimate tensile

strength values. Therefore, annealing treatment of the alloy will be suitable for applications involving high ductility while age hardening treatment will be suitable for applications that require high ultimate tensile strength and yield strength values. In contributing to what is already known, the present study was undertaken to investigate the effect of aging parameters on the mechanical properties of the Be-and/or Zr treated cast and heat-treated 7075 alloys.

Optimizing the results of 7075 Al-Mg-Zn castings obtained from ASTM B-108 type permanent metallic mold casting processes, and incorporating the effects of melt treatments and the effects of heat treatment on the structure (and, hence, on the alloy properties), is expected to provide a better understanding of the metallurgical characteristics of such alloy. By study the impact of Be and /or Zr additions and heat treatments for Al-Mg-Zn (7075) aluminum alloys on the mechanical properties, it is possible to determine conditions necessary to achieve optimum mechanical properties.

Statistical design of experiments (DOE) is a widely known experimentation technique used in such cases, where experiments are carried out to determine the effect of an independent variable on a dependent variable and the relationship between them, using a regression model based on the experimental data. The DOE technique has been applied variously to assist in the production of high quality products, in the economical operation of and stability and reliability of many procedures [21]-[24]. In this technique, a full factorial design is increased by one or more factors/independent variables to be analyzed without increasing the number of experimental runs. In relation to the proposed work, statistical design of experiments (DOE) and fractional factorial design techniques will be applied to the experimental results obtained from these work. Regression equations will be developed between response and control variables to acquire an understanding of the effects of the variables and their interactions on the properties of the alloy studied.

## II. EXPERIMENTAL PROCEDURES AND METHODOLOGY

Experimental 7075 alloy was prepared through the addition of measured amounts of Mg, Zn, Si, Cu, and Fe to the molten aluminum. Table I shows the average chemical composition of the base alloy investigated. Measured Mg, Zn, Si, Cu, Fe and other additions were made to the melt. Alloying elements were added in the form of master alloys or pure metals to obtain the

pre-determined level/levels of each. Prior to casting, the molten metal were degassed for 15min using pure, dry argon to remove the hydrogen and inclusions.

Several experimental alloys were prepared and tensile test bars were cast using an ASTM B-108 type permanent metallic mold that preheated to 450°C. Several sets of test bars corresponding to the base alloy were conventionally heat-treated, where the bars were, then quenched in 65°C warm water, followed by aging at different temperatures for different periods of time up to 100hr (see Table II). All samples are solution heat-treated at 470°C/8h, followed by warm water quenching (65°C).

Tensile testing was carried out for the heat-treated test bars at room temperature using an MTS Servohydraulic mechanical testing machine working at a strain rate of  $1.0 \times 10^{-4}$ /s. The elongation of the test specimens was measured using a strain gauge extensometer attached to the specimen during the tension test. For each sample tested a stress-strain curve was obtained to illustrate the mechanical behavior of each specimen under the applied load. A data acquisition system attached to the MTS machine provided the tensile test data, namely, elongation to fracture, yield strength at 0.2% offset strain and ultimate tensile strength. For each composition, five test bars were tested in the as-cast and heat-treated conditions. The microstructures of the polished sample surfaces were examined using an optical microscope linked to a Clemex image analysis system.

Statistical design of experiments (DOE) and fractional factorial design are efficient, well-established techniques which may be applied to study and control the properties and behavior of an alloy system, where, by developing regression equations between the response variable (mechanical properties) and the factors varied (pre-aging and aging heat treatment parameters, etc.), these equations may be used to predict the alloy processing/heat treatment conditions required to achieve the desired properties.

Ultimate tensile strength, 0.5% offset yield strength and % elongation measurements were performed on all cast and heat-treated specimens prepared from the various 7075 alloys. Experimental correlations of the results obtained from the ultimate tensile strength, 0.5% offset yield strength and % elongation measurements (responses) are analyzed using factorial analysis method through empirical models to establish the relations between these responses and different pre-aging and aging parameters of 7075 alloys (variables). The main factors are Pre-aging Temperature (PA T0C), Pre-aging time (PA t h), Aging temperature (AT0C), Aging time (At h).

Once the responses, factors (6) and levels have been selected, see Table III, the next step is to design the experimental runs. After the parameters and the values input into the software (MINITAB 14), a DOE model will be automatically generated with specific number of runs coupled with specific parametric settings. In this case, 50 runs were generated.

TABLE I  
AVERAGE CHEMICAL COMPOSITION (WT %) OF THE BASE METAL AND THE 7075 ALLOYS

Code	Si	Fe	Mn	Mg	Cu	Zn	Cr	Ti	Sr	Zr	Be	Al
A	0.17	0.38	0.33	2.26	1.98	6.42	0.30	0.016	0.009	0.001	0.000	Bal.
B	0.19	0.40	0.32	2.15	2.02	6.47	0.29	0.013	0.012	0.001	0.024	Bal.
C	0.20	0.47	0.33	2.71	2.22	7.21	0.14	0.016	0.005	0.123	0.017	Bal.

TABLE II

HEAT TREATMENT CONDITIONS FOR BE-CONTAINING 7075 ALLOYS	
Conditions	Aging Heat treatment Description
As-cast	As-cast
SHT	SHT
3-5	T4
6-12	T6
13-19	T6
20-26	T6
27-33	T6
	DA1
	DA2
	DA3
	DA4

TABLE III

EXPERIMENTAL CORRELATION BETWEEN METALLURGICAL PARAMETERS AND ULTIMATE TENSILE STRENGTH (UTS-MPa), 0.2% PROOF YIELDS STRENGTH AND % ELONGATION OF CAST AND HEAT TREATED 7075 ALLOYS: DESIGN OF EXPERIMENT (DOE)- FACTORS AND THEIR UNCODED LEVELS

No.	Parameters	Notation	Unit	Level			
				Encoded		Coded	
				Low	High	Low	High
	Be	A	%	0.024	-1		
	Zr	B	%	0.001	0.123	-1	
	PA T 0C	C	0C			-1	
	PA t h	D	H	24 h	-1		
	AT 0C	E	0C			-1	
	At h.	F	H	24 h	-1		

III. RESULTS AND DISCUSSIONS

A. Al-Mg-Zn-Cu Alloys (7075 Alloys): Effect of Zr and Be

Alloying is one of the effective methods to make high performance cast aluminum alloys. Melt treatments, such as grain refining, improve the casting and mechanical properties of cast Al-Mg-Zn alloys. Chemical modification, using grain refiners creates large numbers of nuclei in melt thereby inducing the formation of small equiaxed grains of Al dendrites. Zirconium is used as a grain refiner to reduce the as cast grain size and consequently to improve strength and ductility [25].

Figs. 1 (a), (b) show the variation in as-cast alloy Ultimate tensile strength (UTS-MPa), 0.2% proof yields strength and % elongation as a function of Zr and/or Be content. Figs. 1 (c), (d) show the One Way ANOVA plots for 0.2% proof yields strength and % elongation data having a confidence level of 95% with different Zr content. While, Figs. 1 (e), (f) show the One Way ANOVA plots for 0.2% proof yields strength and % elongation data having a confidence level of 95% with different Be content. Slight increases in 0.2% proof yields strength with increasing both Zr and Be content are observed in Fig. 1. The reverses are observed in % elongation plots.

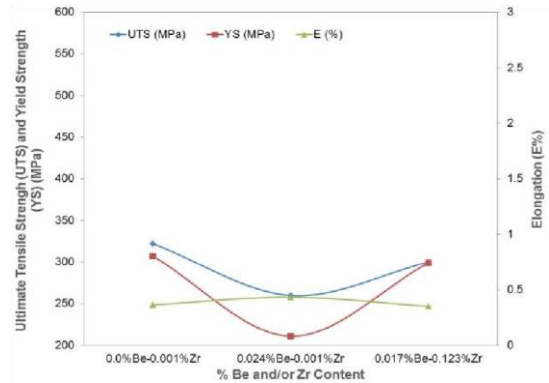


Fig. 1 (a) Effect of %Be and/or Zr on tensile properties of 7075 alloy

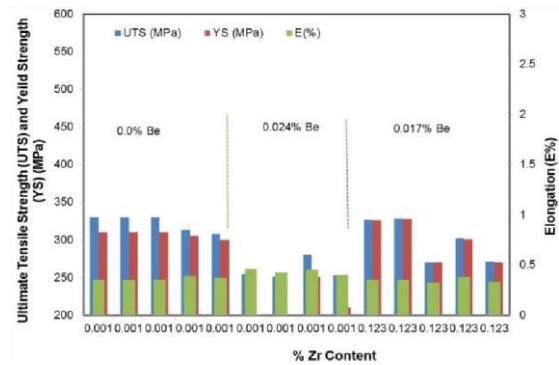


Fig. 1 (b) Effect of % Zr on tensile properties of 7075 alloy at different %Be

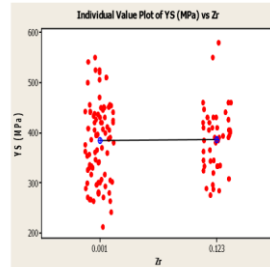


Fig. 1 (c) One Way ANOVA of 0.2% proof yields strength for 7075 alloy with different Zr content

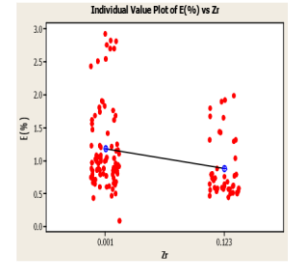


Fig. 1 (d) One Way ANOVA of % elongation for 7075 alloy with different Zr content

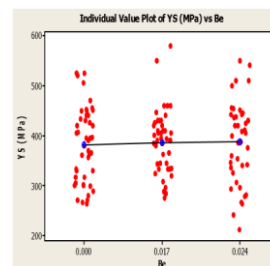


Fig. 1 (e) One Way ANOVA of 0.2% proof yields strength for 7075 alloy with different Be content

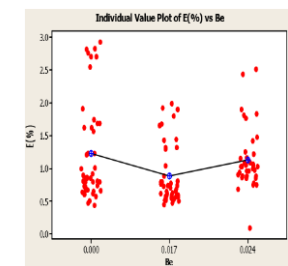


Fig. 1 (f) One Way ANOVA of % elongation for 7075 alloy with different Be content

Fig. 1 Ultimate tensile strength (UTS-MPa), 0.2% proof yields strength and % elongation for as-cast 7075 alloy containing Zr and/or Be

**B. Aging Behavior of Al-Mg-Zn Alloys (7075 Alloys)**

During the early stages of aging of an alloy of Al-Mg-Zn, the saturated solid solution first develops solute clusters. However, the supersaturation of vacancies allows diffusion, thus leading to zone formation, called GP zones. During natural aging (while the alloy is left at room temperature for a sufficiently long time), or aging below the G.P zone solvus line, G.P zones and  $\eta'$  are formed within the matrix. The hardening effect appears to be associated with a strong internal chemical effect, which makes them difficult to be cut by dislocations. The coherency, lattice distortion, and strain field around the G.P zones and  $\eta'$  particles restrict the dislocation motion, leading to an increase in the strength and hardness of the alloy.  $\eta'$  heterogeneously nucleated on dislocations if aging is carried out above the G.P zones solvus line.

Characteristic Feature of quenched and aged Al-Mg-Zn (7xxx) alloys is the presence of (PFZ) adjacent to the grain boundaries. A rapid quench followed by immediate aging would result in a coarse matrix precipitate distribution and a wide PFZ. However, the introduction of a short aging treatment at, say 100°C between quenching and the higher temperature aging would refine the matrix precipitates and produce a narrow PFZ. This is called preaging or duplex aging. However, the interior of grains may develop an acceptable precipitate size and density.

Duplex aging is carried out in two steps: first at relatively low temperature below the G.P zones solvus, and then at a higher temperature. In this way a fine dispersion of G.P zones obtained during the first stage can act as heterogeneous nucleation sites for precipitation at the higher temperature. By this treatment, finer precipitate distributions were obtained than those obtained from the single ageing treatment at the higher temperature. Duplex aging enhances corrosion resistance since the grain boundary zone is removed. The basic idea of all heat treatment is to seed a uniform distribution of stable nuclei at the low temperature which can then be grown to optimum size at the high temperature.

Fig. 2 shows the variation in ultimate tensile strength (UTSMPa), 0.2% proof yields strength and % elongation for different heat treated 7075 Al-Mg-Zn alloys containing Be and/or Zr. The 7075 alloy also demonstrates a high response to age hardening. Fitted line Plots are shown in Figs. 2 (a)-(c) for Ultimate tensile strength (UTS-MPa), 0.2% proof yields strength and % elongation Data when aging is carried out for alloy (A) in the T4 and T6- condition with different temperatures at 24 h. Again, similar results of Fitted line Plots Ultimate tensile strength (UTS-MPa), 0.2% proof yields strength and % elongation for alloy (B) and for alloy (C) are shown in Figs. 2 (d)-(f) and Figs. 2 (j), (h), respectively when T4 and T6-aging (different temperatures) at 24 hours.

From the Data result shown in Fig. 2, Peak values of Ultimate tensile strength (UTS-MPa) and 0.2% proof yields strength are

observed for different alloys when aging was carried out at 120C. On the other hand, a minimum values are observed for % elongation results when aging was carried out at the same temperature.

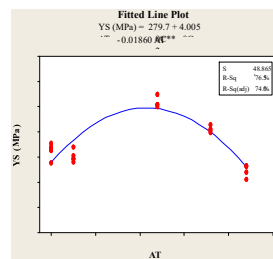
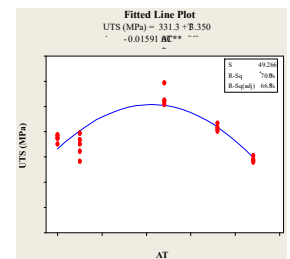
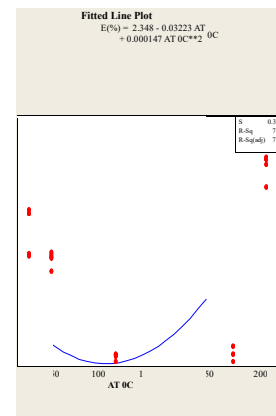
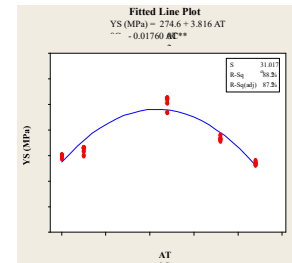
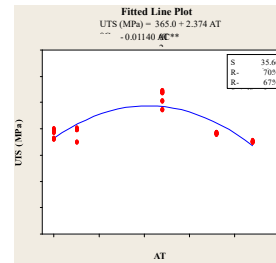


Fig. 2 (c) Fitted line Plots of % elongation for alloy (A).

Fig. 2 (d) Fitted line Plots of Ultimate tensile strength (UTS-MPa) for alloy (B)

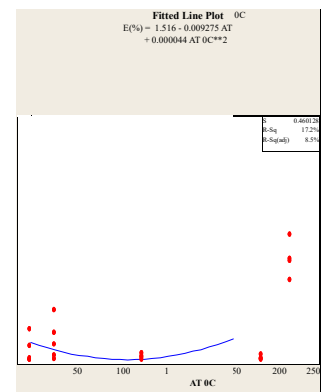


Fig. 2 (a) Fitted line Plots of Ultimate tensile strength (UTS-MPa) for alloy (A)

Fig. 2 (b) Fitted line Plots of 0.2% proof yields strength for alloy (A)

Fig. 2 (e) Fitted line Plots of 0.2% proof yields strength for alloy (B)

Fig. 2 (f) Fitted line Plots of % elongation for alloy (B)

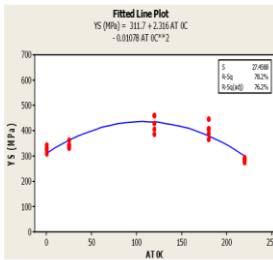


Fig. 2 (j) Fitted line Plots of 0.2% proof yields strength for alloy (C)

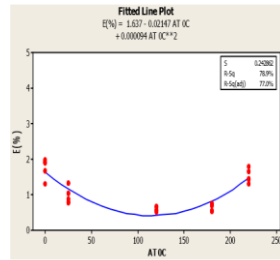


Fig. 2 (h) Fitted line Plots of % elongation for alloy (C)

Fig. 2 Fitted line Plots of Ultimate tensile strength (UTS-MPa), 0.2% proof yields strength and % elongation for alloys (A, B and C) when aging are carried out at different temperatures at 24h

### C. Experimental Correlation between Metallurgical Parameters and Mechanical Properties of 7075 Aluminum Alloys

An attempt has been made to quantify the effects of Be%, Zr%, pre-aging and aging parameters on the ultimate tensile strength (UTS-MPa), 0.2% proof yields strength and % elongation of cast Al-Mg-Zn alloys. An understanding of these parameters would help in selecting the metallurgical conditions required to achieve the optimum mechanical properties. Ultimate tensile strength (UTS-MPa), 0.2% proof yields strength and % elongation measurements were carried out on specimens prepared from 7075 alloys in the cast and heat-treated conditions. Experimental correlations of the results obtained from the Ultimate tensile strength (UTSMPa), 0.2% proof yields strength and % elongation results measurements are analyzed. Models that relate heat treatment parameters to the Ultimate tensile strength (UTS-MPa), 0.2% proof yields strength and % elongation of such alloys are developed in the present study.

Experimental correlations of the results obtained from the mechanical testing measurements are analyzed through empirical models to establish the relations between the ultimate tensile strength, 0.5% offset yield strength and % elongation and %Be, %Zr, pre-aging and aging parameters of 7075 alloys. The main factors are %Be, %Zr, Pre-aging Temperature (PA T0C), Pre-aging time (PA t h), Aging temperature (AT0C), Aging time (At h). Once the responses, factors (6) and levels have been selected, see Table III, the next step is to design the experimental runs. After the parameters and the values input into the software (MINITAB 14), a DOE model will be automatically generated with specific number of runs coupled with specific parametric settings. In this case, 130 runs were generated.

#### 1. Regression Analysis

In this experimental study, an empirical model was developed through the regression analysis to correlate the metallurgical parameters to the response Ultimate tensile strength (UTS-MPa), 0.2% proof yields strength and % elongation. The estimated regression coefficients in Ultimate tensile strength (UTS-MPa), 0.2% proof yields strength and % elongation regression equations (Refer to (1) -(3)) shows that the following parameters; i.e., Pre-aging time (PA t h), Aging time (At h) and Aging Temperature (AT 0C), has noteworthy influence on the Ultimate tensile strength (UTS-MPa) and 0.2% proof yields strength. The p – value for these parameters shows that the values are below the

accepted value of 0.05. For Ultimate tensile strength (UTS-MPa) and 0.2% proof yields strength regression model, The R – Sq value given is 15.4% and 25.4%, respectively. On the other hand The R – Sq value for the % elongation regression model is 43.2% and both of the pre-aging time (PA t h) and Aging Temperature (AT 0C) as well as the % Zr have a significant effect on the % elongation. The p – value for these parameters shows that the values are below the accepted value of 0.05.

$$\text{UTS (MPa)} = 390 - 450 \text{ Be} - 16.1 \text{ Zr} - 0.101 \text{ PA T 0C} \\ (1) + 1.16 \text{ PA t h} + 0.0664 \text{ AT 0C} + 1.89 \text{ At h.}$$

$$\text{YS (MPa)} = 320 + 161 \text{ Be} + 16 \text{ Zr} - 0.0724 \text{ PA T 0C} + (2) 2.12 \\ \text{PA t h} + 0.232 \text{ AT 0C} + 1.74 \text{ At h.}$$

$$\text{E(\%)} = 1.81 - 3.60 \text{ Be} - 2.36 \text{ Zr} + 0.000432 \text{ PA T 0C} - (3) \\ 0.0177 \text{ PA t h} - 0.00356 \text{ AT 0C} - 0.00295 \text{ At h.}$$

#### 2. Mathematical Model (Factorial DOE and ANOVA Results)

Mathematical model (Refer to (4)) are developed to relate the % elongation with the different metallurgical parameters (as mentioned above) to acquire an understanding of the effect of the variables and their interactions on the ductility of 7075 Al-alloys containing Be- and/or Zr. The design of experiment (DOE) Factorial Plots (main effect plot and interaction effect plot) and analysis of variance (ANOVA) is conducted and the results are shown in Figs. 3 and 4.

Figs. 3 (a), (b) show the Pareto chart of the standardized effects and Normal Probability plot for the % elongation data having a confidence level of 95%. Figs. 3 (c)-(e) show the main effects plot (Factorial Plots) for the mean values of the Ultimate tensile strength (UTS-MPa), 0.2% proof yields strength and % elongation data in terms of the same parameters. However, Figs. 3 (f)-(h) show the interaction plot for the mean values of the Ultimate tensile strength (UTSMPa), 0.2% proof yields strength and % elongation data in terms of different combination of factors. On the other hand, Analysis of Variance (ANOVA) Plots (main effect plot and interaction effect plot) are shown in Fig. 4. Figs. 4 (a)-(c) show the main effects plot (ANOVA Plots) for the mean values of the Ultimate tensile strength (UTS-MPa), 0.2% proof yields strength and % elongation data in terms of the same parameters. However, Figs. 4 (d)-(f) show the interaction plot for the mean values of the Ultimate tensile strength (UTSMPa), 0.2% proof yields strength and % elongation data in terms of different combination of factors.

#### 3. Factorial Fit (Elongation Model)

In the predicted model (Refer to (4)), within the variation range of the variables studied, the most significant effects is correspond to the Aging Temperature (AT), Pre-aging temperature (PA T0C), the interaction between Pre-aging temperature (PA T0C) and Pre-aging time (PA t h) and the interaction between Be and Pre-aging time (PA t h). The effects of the other coefficients however, were found to be insignificant. From the values under the estimated effects coefficients, it is observed that four parameters; has

noteworthy influence on the %elongation. Any P-values are below the accepted value of 0.05 have influence on the %elongation, On the other hand, the p – values above the accepted value of 0.05 can be considered to have no influence on the % elongation to some extent. The R – Sq value given is 55.06%.

$$\begin{aligned}
 E(\%) = & 2.268 - 34.6 * Be\% + 0.37 * Zr\% - \\
 & 0.00665 * PA T OC - 0.0421 * PA t h - \\
 & 0.00286 * AT OC - 0.01595 * At h - \\
 & 0.0094 * Be * PA T OC + 1.215 * Be * \\
 & PA t h + \\
 & 0.0539 * Be * AT OC + \\
 & 0.639 * Be * At h 0.00225 \\
 & * Zr * PA T OC - 0.157 * \\
 & Zr * PA t h + \\
 & 0.0055 * Zr * AT OC + 0.0476 * Zr * \\
 & At h + \\
 & 0.000355 * PA T OC * PA t h - \\
 & 4.70928E - 06 * PA T OC * AT OC
 \end{aligned}
 \tag{4}$$

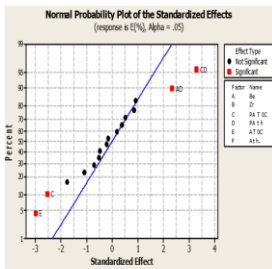


Fig. 3 (a) Normal Probability plot of the standardized effects for the % elongation

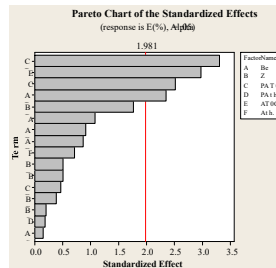


Fig. 3 (b) Pareto chart of the standardized effects for the % elongation

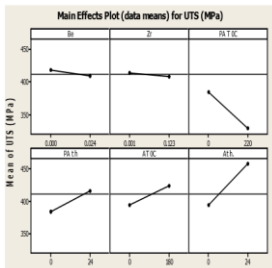
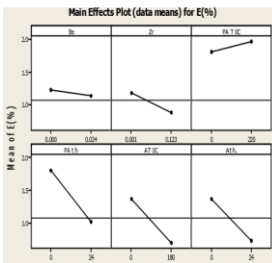


Fig. 3 (c) Main effects plot for the mean values of Ultimate tensile strength (UTS-MPa)



Elongation

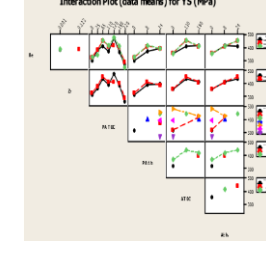
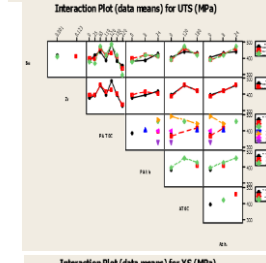
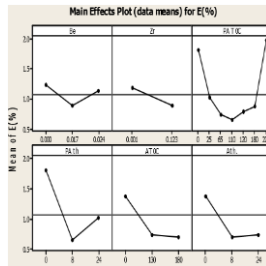


Fig. 3 (e) Main effects plot for the mean values of % elongation

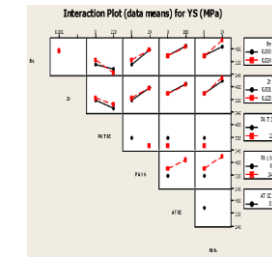


Fig. 3 (g) Interaction plot for the mean values of 0.2% proof strength elongation

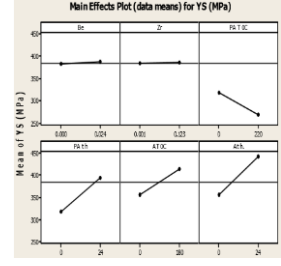


Fig. 3 (d) Main effects plot for the mean values of 0.2% proof yields strength

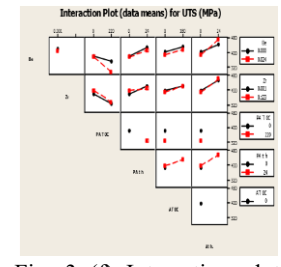


Fig. 3 (f) Interaction plot for the mean values of Ultimate tensile strength (UTS-MPa)



Fig. 3 (h) Interaction plot for the mean values of % yields strength elongation

Fig. 3 Factorial Plots (main effect plot and interaction effect plot) for the Ultimate tensile strength (UTS-MPa), 0.2% proof strength and % elongation data in terms of % Be, % Zr, pre-aging and aging parameters (Temperature and time)

Fig. 4 (a) Main effects plot for the mean values of Ultimate tensile strength (UTS-MPa)

Fig. 4 (b) Main effects plot for the mean values of 0.2% proof yields strength

Fig. 4 (c) Main effects plot for the mean values of % elongation

Fig. 4 (d) Interaction plot for the mean values of Ultimate tensile strength (UTS-MPa)

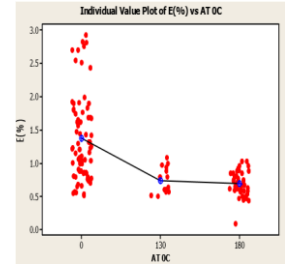
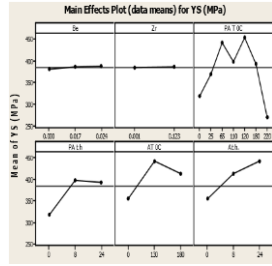
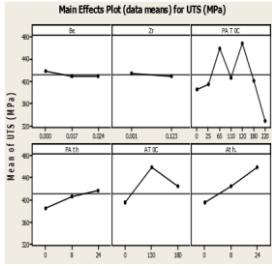


Fig. 4 (e) Interaction plot for the mean values of 0.2% proof yields

Fig. 4 (f) Interaction plot for the mean values of % elongation

Fig. 5 (b) One Way ANOVA of % elongation with aging temperature

Fig. 4 ANOVA Plots (main effect plot and interaction effect plot) for the mean values of Ultimate tensile strength (UTS-MPa), 0.2% proof yields strength and % elongation data in terms of % Be, % Zr, pre-aging and aging parameters (Temperature and time)

Fig. 5 (d) One Way ANOVA of % elongation with aging time

4. One Way ANOVA

One way ANOVA for 0.2% proof yields strength and %elongation data results having a confidence level of 95% with different pre-aging, aging parameters (Time and Temperature) are shown in Fig.5 for heat treated 7075 Al-MgZn alloy. Figs. 5 (a),

(c) show the results for the 0.2% proof yields strength as a function of Aging temperature and aging time, respectively. On the other hand Figs. 5 (b), (d) show the results of % elongation as a function of the same parameters. Figs. 5 (e), (g) show the results for the 0.2% proof yield strength as a function of Pre-aging temperature and Pre-aging time, respectively. On the other hand Figs. 5 (f), (h) show the results of % elongation as a function of the same parameters. It is observed from Fig. 5 that an increase in alloy strength is accompanied by a reduction in alloy ductility.

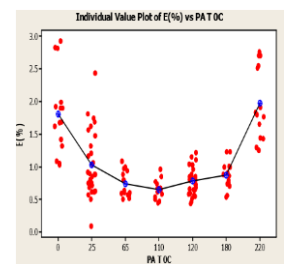


Fig. 5 (e) One Way ANOVA of 0.2% proof yields strength with pre-aging temperature

Fig. 5 (f) One Way ANOVA of % elongation with pre-aging temperature

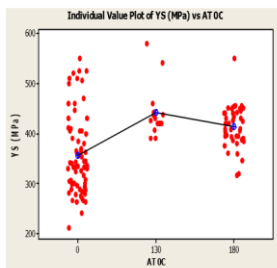


Fig. 5 (a) One Way ANOVA of 0.2% proof yields strength with aging temperature

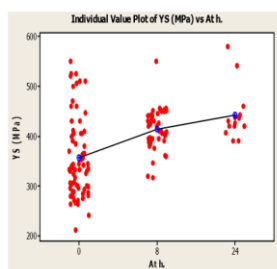


Fig. 5 (c) One Way ANOVA of 0.2% proof yields strength with aging time

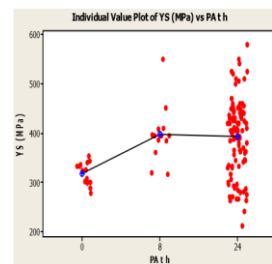
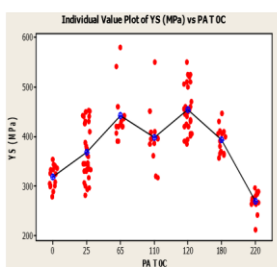


Fig. 5 (g) One Way ANOVA of 0.2% proof yields strength with pre-aging time

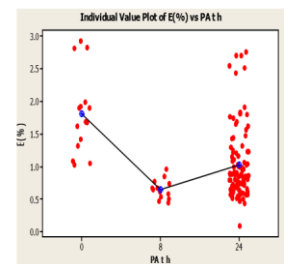


Fig. 5 (h) One Way ANOVA of % elongation with pre-aging time

Fig. 5 One Way ANOVA of 0.2% proof yields strength and % elongation data having a confidence level of 95% with different aging and pre-aging parameters (Time and Temperature)

5. Response Surface Methodology

Response surface methodology is used to investigate the relationship between metallurgical parameters with the mechanical properties of Al-Mg-Zn-Cu alloys. Fig. 6 shows the contour plots of ultimate tensile strength, 0.2% proof yields strength and % elongation at various combination values of metallurgical parameters.

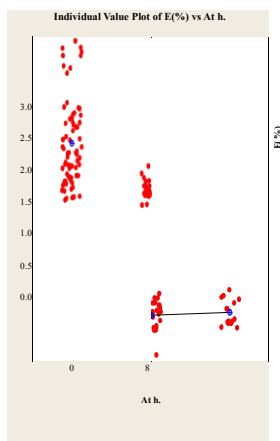


Fig. 6 (a) Contour Plots of 0.2% proof yields strength at different pre-aging temperature and time

Fig. 6 (b) Contour Plots of % elongation at different levels of Be and Zr

International Science Index, Materials and Metallurgical Engineering Vol:9, No:1, 2015 waset.org/Publication/10000583

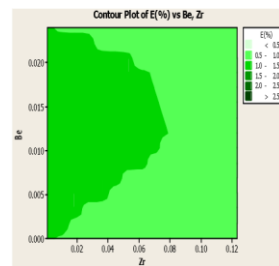
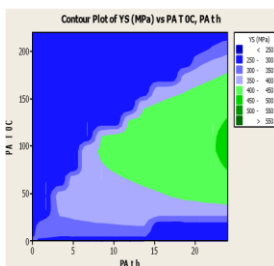
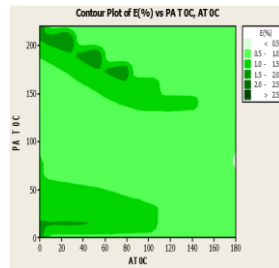
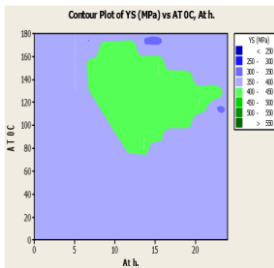


Fig. 6 (c) Contour Plots of 0.2% proof yields strength at different aging temperature and time

Fig. 6 (d) Contour Plots of % elongation at different aging temperature and pre-aging temperatures

Fig. 6 Contour Plots of 0.2% proof yields strength and % elongation at various combination values of different metallurgical conditions

*D. Microstructure of 7075 Alloys*

The microstructure of as cast, SHT and Aged Al-Zn-Mg alloys are shown in Fig. 7. This structure was obtained from the ingot

International Science Index, Materials and Metallurgical Engineering Vol:9, No:1, 2015 waset.org/Publication/1000058

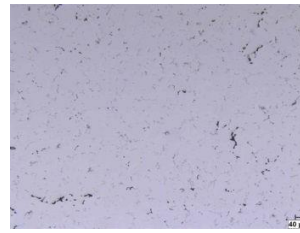


Fig. 7 (a) Optical micrograph of as-cast 7075 (alloy A)



Fig. 7 (c) Optical micrograph of as-cast 7075 (alloy C)

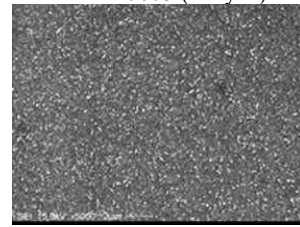


Fig. 7 (e) Optical micrograph of as-aged 7075 (alloy B) when aging at 120C for 24hr

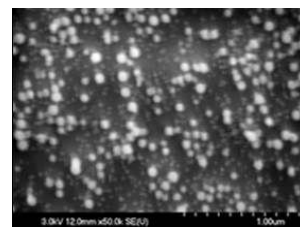


Fig. 7 (b) Optical micrograph of as-cast 7075 (alloy B)



Fig. 7 (b) Optical micrograph of as-cast 7075 (alloy B)



Fig. 7 (d) Optical micrograph of as-SHT 7075 (alloy B)

which has been cooled quickly to obtain equi-axed network structure. This network structure is made up of particles of several intermetallic compounds formed by combinations of the alloying elements in this alloy. Some of these compounds are soluble while others have slight or practically insolubility. A dendritic microstructure is apparent in all micrographs. Figs. 7 (a)-(c) show a micrograph for as cast microstructure with different magnifications. Microstructure appears in Fig. 7 (d) for Solution heat treatment. During the solution treatment, the alloy constituents were dissolved. Microstructures when aging at different temperature at 24 hour are shown in Figs. 7 (e)-(h).

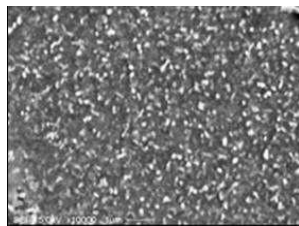


Fig. 7 (f) Optical micrograph of as-aged 7075 (alloy B) when aging at 150C for 24hr

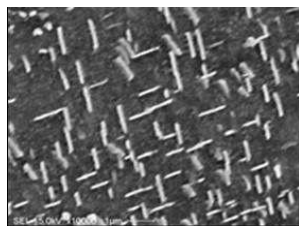


Fig. 7 (h) Optical micrograph of as-aged 7075 (alloy B) when aging at 220C for 24hr

Fig. 7 (g) Optical micrograph of as-aged 7075 (alloy B) when aging at 180C for 24hr

Fig. 7 Optical micrograph (a, b and C) microstructure of as-cast, SHT and aged 7075 alloys (alloy A, C and B)

#### IV. CONCLUSIONS

1. Aging at room temperature resulted in slight increase in the alloy strength reaching about 400MPa after aging for 192h.
2. Peak values of Ultimate tensile strength (UTS-MPa) and 0.2% proof yields strength are observed for 7075 alloys when aging was carried out at 120C. On the other hand, minimum values are observed for % elongation results.
3. Mathematical and regressions models for calculation of mechanical properties (i.e. % elongation) in terms of %Be, % Zr, Pre-Aging Time (h), Pre-Aging Temp (C) Aging Time (h) and Aging Temp (C) are developed.
4. The Ductility of Al-Mg-Zn-Cu alloys increases with (the interaction between Pre-aging temperature (PA T0C) and Pre-aging time (PA t h) and the interaction between Be and Pre-aging time (PA t h)) and decrease with (Aging Temperature (AT), Pre-aging temperature (PA T0C)).

#### REFERENCES

- [1] T.D. Rostova, V.G. Davydov, V.I. Yelagin, and V.V. Zakharov, *Materials Science Forum*, 331-337 (2000) 793-798.
- [2] F.A. Costello, J.D. Robson and P.B. Prangnell, *Mater. Sci. Forum*, 396402 (2002) 757-762.
- [3] J.D. Robson and P.B. Prangnell, *Mater. Sci. Technol.*, 18 (2002) 607.
- [4] B. Morere, C. Maurice, R. Shahani, and J. Driver, *Met.Mater.Trans.A.*, 32A (2001) 625.
- [5] Y.W. Riddle and T.H. Sanders Jr., *Materials Science Forum*, 331-337 (2000) 939-944.

- [6] W.V. Youdelis and W. Fang "Effect of beryllium on age hardening, defect structure, and S' formation in Al-2.5Cu-1.2Mg alloy", *Materials Science and Technology*, Volume 10, Issue 12 (01 December 1994), pp. 1031-1043.
- [7] T. Xiao; W. V. Youdelis "Effect of beryllium and calcium on aging behaviour of Al-0.75Mg-0.5Si alloy" *Materials Science and Technology*, Volume 5, Issue 10 (01 October 1989), pp. 991-994.
- [8] Paih-Shiang Wang, Sheng-Long Lee, Jing-Chie Lin and Min-Ten Jahn "Effects of solution temperature on mechanical properties of 319.0 aluminum casting alloys containing trace beryllium", *Journal of Materials Research*, Vol. 15, Issue 09, 2000, pp 2027-2035.
- [9] I.J. Polmear, "Recent Developments in Light Alloys," *Materials Transactions, JIM*, 37(1) (1996), 12-31.
- [10] H.Y. Hunsicker, "Development of Al-Zn-Mg-Cu Alloys for Aircraft," *Proceeding Rosenhain Century Conference, Metals Society*, London, (1976), 359-376.
- [11] J.T. Staley, "History of Wrought-Aluminium-Alloy Development," *Aluminium Alloys: Contemporary Research and Applications, Treaties on Materials Science and Technology*, Academic Press, 31 (1989), 3-31.
- [12] Patent No. EP037779B2, "Aluminum Alloy Product Having Improved Combinations of Strength, toughness and Corrosion Resistance," New European Patent Specification, Bulletin 2001/36, 5 September 2001.
- [13] N.E. Paton and A.W. Sommer, "Influence of Thermomechanical Processing Treatments on Properties of Aluminum Alloys," *Proceeding Third international Conference on Strength of Metals and Alloys, Metals Society*, London, 1 (1973), 101-108.
- [14] A. Yamamoto et al., "Calorimetric and Resistivity Study of formation and Redissolution of Precipitates in 7050 Aluminum Alloy," *Materials Transactions, JIM*, 39 (1) (1998), 69-74.
- [15] A. Joshi, C.R. Shastry and M. Levy, "Effect of Heat Treatment on Solute Concentration at Grain Boundaries in 7075 Aluminum Alloy," *Metallurgical Transactions A*, 12 (A) (1981), 1081-1088.
- [16] M.E. Fine, "Precipitation Hardening of Aluminum Alloys," *Metallurgical Transactions A*, 6 (A) (1975), 625-630.
- [17] J.K. Park and A.J. Ardell, "Microstructures of the Commercial 7075 Al Alloy in the T651 and T7 Tempers," *Metallurgical Transactions A*, 14 (A) (1983), 1957-1965.
- [18] A. Karaaslan, I. Kaya and H. Atapek, "Effect of Aging Temperature and of Retrogression Treatment Time on the Microstructure and Mechanical Properties of Alloy AA 7075," *Metal Science and Heat Treatment*, 49 (9-10) (2007), 443-447.
- [19] J.K. Park and A.J. Ardell, "Effect of Retrogression and Reaging treatments on the Microstructure of Al-7075-T651," *Metallurgical Transactions A*, 15 (A) (1984), 1531- 1543.
- [20] Montgomery, D. (1991), *Design and analysis of experiments*, 3rd Edn., 270-569, New York, John Wiley & Sons.
- [21] Berthouex, P., Brown, L. (2002), *Statistics for environmental engineers*, 2nd Edn, 185-276, New York, Lewis Publishers.
- [22] Hatch, J.E. (Ed.), *Aluminium Properties and Physical Metallurgy*, 1 st.